

# Direction Finding Based on Spatial Time-Frequency Distribution Matrices<sup>1</sup>

Moeness G. Amin and Yimin Zhang

Department of Electrical and Computer Engineering, Villanova University, Villanova, Pennsylvania 19085

E-mail: [moeness@ece.vill.edu](mailto:moeness@ece.vill.edu), [yimin@ieee.org](mailto:yimin@ieee.org)

---

Amin, Moeness G., and Zhang, Yimin, Direction Finding Based on Spatial Time-Frequency Distribution Matrices, *Digital Signal Processing* **10** (2000), 325–339.

Spatial time-frequency distributions (STFDs) have been recently introduced as the natural means to deal with source signals that are localizable in the time-frequency domain. It has been shown that improved estimates of the signal and noise subspaces are achieved by constructing the subspaces from the time-frequency signatures of the signal arrivals rather than from the data covariance matrices, which are commonly used in conventional subspace estimation methods. This paper discusses the application of STFD to high-resolution direction finding. We focus on both the role and the effect of crossterms in angle estimation when multiple time-frequency points are incorporated. Simulation examples are presented to compare the performance of joint block-diagonalization and time-frequency averaging techniques for incorporating multiple autoterm and crossterm points in subspace estimation. © 2000 Academic Press

*Key Words:* spatial time-frequency distribution; direction finding; cross-term distribution; array signal processing.

---

## 1. INTRODUCTION

In many signal processing applications, the multidimensional signal is directly utilized to estimate some signal parameters, such as the number of sources and their directions of arrival [1, 2]. Subspace-based methods use a geometrical relation involving the exact moments of the data. The desired signal parameters are extracted by solving this relation in some approximate sense and by using sample moments instead of the exact ones. The commonly applied eigenstructure subspace methods assume stationary signals. When the frequency content of the measured data is time-varying, the performance of

<sup>1</sup> This work was supported by the Office of Naval Research under Grant N00014-98-1-0176.



these methods can be significantly improved by proper use of the data time-frequency characteristics.

The evaluation of quadratic time-frequency distributions of the data snapshots across the array yields spatial time-frequency distributions (STFDs) which are most appropriate to handle sources of nonstationary waveforms that are highly localized in the time-frequency domain [3, 4, 9]. Spreading the noise power while localizing the source energy in the time-frequency domain amounts to increasing the robustness of eigenstructure signal and noise subspace estimation methods with respect to channel and receiver noise and hence improves resolution and signal separation performance.

In this paper, we consider the applications of spatial time-frequency distributions to the direction finding problem. In [4], the time-frequency MUSIC (t-f MUSIC) was introduced. In [9], the subspace analysis for the time-frequency distribution matrices is presented, and the performance of the time-frequency MUSIC is analyzed. The time-frequency maximum likelihood (t-f ML) for direction finding has also been introduced and analyzed [8]. However, these results were obtained under the assumption that only the autoterms of STFDs are considered for STFD matrix construction. The effect of crossterms on direction-of-arrival (DOA) estimations has not been made clear. In this paper, we focus on the performance of the t-f MUSIC when crossterms are incorporated. The main contribution of this paper is not based on improved distinction between auto- and crossterms but rather we examine the effect on performance when each or both of these terms are allowed to take part in matrix and STFD problem formulation. For the cases where it is difficult to discriminate between distribution terms, then it is likely that both auto- and crossterms will be considered, which is a case discussed and simulated in this paper.

This paper is organized as follows. Section 2 introduces the signal model and gives a brief review of the definition and properties of the spatial time-frequency distributions. In Section 3, the time-frequency MUSIC algorithm is briefly discussed. In Section 4, we consider the effect of crossterms to direction finding. Simulation examples are presented to examine the effect of crossterms, and a comparison between joint block-diagonalization and time-frequency averaging is performed.

## 2. SPATIAL TIME-FREQUENCY DISTRIBUTIONS

### 2.1. Signal Model

In narrowband array processing, when  $n$  signals arrive at an  $m$ -element array, the linear data model

$$\mathbf{x}(t) = \mathbf{y}(t) + \mathbf{n}(t) = \mathbf{A}\mathbf{d}(t) + \mathbf{n}(t) \quad (1)$$

is commonly used, where  $\mathbf{A}$  is the mixing matrix of dimension  $m \times n$ ,  $\mathbf{x}(t) = [x_1(t), \dots, x_m(t)]^T$  is the sensor array output vector, and  $\mathbf{d}(t) = [d_1(t), \dots, d_n(t)]^T$  is the source signal vector. The superscript  $T$  denotes the transpose operator. In

direction finding problems, the DOAs of the source signals  $\Theta = [\theta_1, \dots, \theta_n]^T$  are of interest, and the mixing matrix takes the form of  $\mathbf{A}(\Theta) = [\mathbf{a}(\theta_1), \dots, \mathbf{a}(\theta_n)]$ , where  $\mathbf{a}(\theta_i)$  is the  $i$ th steering vector with known structure. On the other hand, in blind source separation application, it is often assumed that the array manifold is unknown and the mixing matrix is not finitely parameterized.  $\mathbf{n}(t)$  is an additive noise vector whose elements are modeled as stationary, spatially and temporally white, zero-mean complex random processes, independent of the source signals. That is,

$$E[\mathbf{n}(t + \tau)\mathbf{n}^H(t)] = \sigma\delta(\tau)\mathbf{I} \quad \text{and} \quad E[\mathbf{n}(t + \tau)\mathbf{n}^T(t)] = \mathbf{0} \quad \text{for any } \tau, \quad (2)$$

where  $\delta(\tau)$  is the Dirac delta function,  $\mathbf{I}$  denotes the identity matrix,  $\sigma$  is the noise power at each sensor, the superscript  $H$  denotes conjugate transpose, and  $E(\cdot)$  is the statistical expectation operator.

In Eq. (1), it is assumed that the number of sensors is higher than the number of sources, i.e.,  $m > n$ . Further, matrix  $\mathbf{A}$  is full column rank, which implies that the steering vectors corresponding to  $n$  different angles of arrival are linearly independent. The spatial correlation matrix is given by

$$\mathbf{R}_{\mathbf{xx}} = E[\mathbf{x}(t)\mathbf{x}^H(t)] = \mathbf{A}\mathbf{R}_{\mathbf{dd}}\mathbf{A}^H + \sigma\mathbf{I}, \quad (3)$$

where  $\mathbf{R}_{\mathbf{dd}} = E[\mathbf{d}(t)\mathbf{d}^H(t)]$  is the signal correlation matrix. We assume that  $\mathbf{R}_{\mathbf{xx}}$  is nonsingular and the observation period consists of  $N$  snapshots with  $N > m$ .

## 2.2. Spatial Time-Frequency Distributions

The STFDs based on Cohen's class of time-frequency distribution were introduced in [3]. The discrete form of Cohen's class of time-frequency distribution of a signal  $x(t)$  is given by [5]

$$D_{xx}(t, f) = \sum_{k=-\infty}^{\infty} \sum_{\tau=-\infty}^{\infty} \phi(k, \tau)x(t+k+\tau)x^*(t+k-\tau)e^{-j4\pi f\tau}, \quad (4)$$

where  $\phi(k, \tau)$  is the time-frequency kernel and the superscript  $*$  denotes complex conjugate. The spatial time-frequency distribution matrix is obtained by replacing  $x(t)$  by the data snapshot vector  $\mathbf{x}(t)$ ,

$$\mathbf{D}_{\mathbf{xx}}(t, f) = \sum_{k=-\infty}^{\infty} \sum_{\tau=-\infty}^{\infty} \phi(k, \tau)\mathbf{x}(t+k+\tau)\mathbf{x}^H(t+k-\tau)e^{-j4\pi f\tau}. \quad (5)$$

Substituting (1) into (5), we can extend  $\mathbf{D}_{\mathbf{xx}}$  to the following form,

$$\mathbf{D}_{\mathbf{xx}}(t, f) = \mathbf{D}_{\mathbf{yy}}(t, f) + \mathbf{D}_{\mathbf{yn}}(t, f) + \mathbf{D}_{\mathbf{ny}}(t, f) + \mathbf{D}_{\mathbf{nn}}(t, f). \quad (6)$$

Under the uncorrelated signal and noise assumption and the zero-mean noise property, it is obvious that  $E[\mathbf{D}_{\mathbf{yn}}(t, f)] = E[\mathbf{D}_{\mathbf{ny}}(t, f)] = \mathbf{0}$ , and it follows

$$E[\mathbf{D}_{\mathbf{xx}}(t, f)] = \mathbf{D}_{\mathbf{yy}}(t, f) + E[\mathbf{D}_{\mathbf{nn}}(t, f)] = \mathbf{A}\mathbf{D}_{\mathbf{dd}}(t, f)\mathbf{A}^H + E[\mathbf{D}_{\mathbf{nn}}(t, f)]. \quad (7)$$

Equation (7) is similar to Eq. (3) which has been commonly used in DOA estimation and blind source separation problems, relating the signal correlation matrix to the data spatial correlation matrix. In the above formulation, however, the correlation matrices are replaced by the spatial time-frequency distribution matrices. This implies that key problems in various applications of array processing, specifically those dealing with nonstationary signal environments, can be approached using bilinear transformations.

It is noted that the relationship (7) holds true for every  $(t, f)$  point. In order to reduce the effect of noise and ensure the full column rank property of the STFD matrix, we consider multiple time-frequency points. Joint block-diagonalization [6, 13] and time-frequency averaging [7, 9] represent the two approaches that have been used for this purpose.

The aforementioned fact of incorporating multiple time-frequency points permits the selection of specific time-frequency regions and as such perform array processing for a subclass of signals. For example, consider the two sources  $A$  and  $B$  to be incident on a multisensor array. As shown in Fig. 1, we assume that source  $A$  occupies the time-frequency region  $R_a$ , where source  $B$  occupies the time-frequency region  $R_b$ . The time-frequency signatures of the two sources overlap, but each source still has a time-frequency region that is not intruded over by the other source. Therefore, when we select  $(t, f)$  points of the region  $R_a \cap \overline{R_b}$ , only signal  $A$  will be involved. The performance improvement is specially significant for closely spaced signals [10].

When  $n_o$  source signals are selected out of the  $n$  signals based on their time-frequency signatures, (7) becomes

$$E[\mathbf{D}_{\mathbf{xx}}(t, f)] = \mathbf{A}^o \mathbf{D}_{\mathbf{dd}}^o(t, f) (\mathbf{A}^o)^H + E[\mathbf{D}_{\mathbf{nn}}(t, f)], \quad (8)$$

where  $\mathbf{A}^o$  and  $\mathbf{D}_{\mathbf{dd}}^o(t, f)$ , respectively, denote the mixing matrix and the source signal TFD matrix defined using the selected  $n_o$  signals.

It is important to note that with the ability to construct the STFD matrix from one or few signal arrivals, the well-known  $m > n$  condition on source localization using arrays can be relaxed to  $m > n_o$ . That is to say, we can perform direction

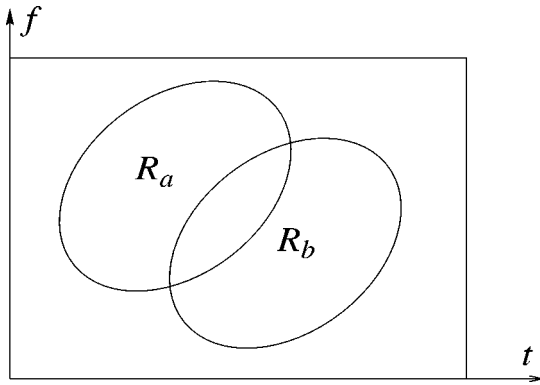


FIG. 1. Signals with different time-frequency signatures.

finding or source separation with the number of array sensors smaller than the number of impinging signals.

### 2.3. Properties

Below, we focus on frequency modulation (FM) signals, modeled as

$$\mathbf{d}(t) = [d_1(t), \dots, d_n(t)]^T = [D_1 e^{j\psi_1(t)}, \dots, D_n e^{j\psi_n(t)}]^T, \tag{9}$$

where  $D_i$  and  $\psi_i(t)$  are the fixed amplitude and time-varying phase of the  $i$ th source signal. For each sampling time  $t$ ,  $d_i(t)$  has an instantaneous frequency (IF)  $f_i(t) = d\psi_i(t)/(2\pi dt)$ .

The consideration of FM signals is motivated by their simplicity as well as the fact that these signals are uniquely characterized by their instantaneous frequencies, and therefore, they have clear time-frequency signatures that can be utilized by the STFD approach.

Consider a simple case in which the FM signals are mutually uncorrelated over the observation period and their respective time-frequency signatures do not overlap, i.e.,

$$\frac{1}{N} \sum_{k=1}^N d_i(k) d_j^*(k) = 0 \quad \text{for } i \neq j, i, j = 1, \dots, n, \tag{10}$$

then the signal correlation matrix in (3) is

$$\mathbf{R}_{\mathbf{d}\mathbf{d}} = \text{diag}[D_1^2, D_2^2, \dots, D_n^2],$$

where  $\text{diag}[\cdot]$  is the diagonal matrix formed with the elements of its vector valued arguments.

We consider pseudo Wigner–Ville distribution (PWVD) as an example of Cohen’s class here. The spatial pseudo-Wigner–Ville distribution (SPWVD) matrix, using a rectangular window of odd length  $L$ , is

$$\mathbf{D}_{\mathbf{x}\mathbf{x}}(t, f) = \sum_{\tau=-(L-1)/2}^{(L-1)/2} \mathbf{x}(t + \tau) \mathbf{x}^H(t - \tau) e^{-j4\pi f \tau}. \tag{11}$$

Assuming that the third-order derivative of the phase is negligible over the window length  $L$ , then along the true time-frequency points of the  $i$ th signal,  $f_i(t) = d\psi_i(t)/(2\pi dt)$ , and  $\psi_i(t + \tau) - \psi_i(t - \tau) - 4\pi f_i \tau = 0$ . Accordingly, the  $i$ th diagonal element of PWVD matrix  $\mathbf{D}_{\mathbf{d}\mathbf{d}}(t, f)$  becomes

$$D_{d_i d_i}(t, f_i) = \sum_{\tau=-(L-1)/2}^{(L-1)/2} D_i^2 = L D_i^2. \tag{12}$$

On the other hand, under the spatial white and temporal white assumptions, the statistical expectation of the noise STFD matrix  $\mathbf{D}_{\mathbf{nn}}(t, f)$  is

$$E[\mathbf{D}_{\mathbf{nn}}(t, f)] = \sum_{\tau=-(L-1)/2}^{(L-1)/2} E[\mathbf{n}(t + \tau)\mathbf{n}^H(t - \tau)]e^{-j4\pi f\tau} = \sigma\mathbf{I}. \tag{13}$$

Therefore, when selecting the time-frequency points along the time-frequency signature or the IF of an FM signal, the SNR of model (7) is  $LD_i^2/\sigma$ , which has an improved factor  $L$  over the one associated with model (3).

The PWVD of each FM source has a constant value over the observation period, providing that we leave out the rising and falling power distributions at both ends of the data record. For convenience of analysis, we select those  $N - L + 1$  time-frequency points of constant distribution value for each source signal. Therefore, the averaged STFD over the time-frequency signatures of  $n_o$  sources, i.e., a total of  $n_o(N - L + 1)$  time-frequency points, is given by

$$\hat{\mathbf{D}} = \frac{1}{n_o(N - L + 1)} \sum_{q=1}^{n_o} \sum_{i=1}^{N-L+1} \mathbf{D}_{\mathbf{xx}}(t_i, f_{q,i}), \tag{14}$$

where  $f_{q,i}$  is the instantaneous frequency of the  $q$ th signal at the  $i$ th time sample. The expectation of the averaged STFD matrix is

$$\mathbf{D} = E[\hat{\mathbf{D}}] = \frac{L}{n_o} \mathbf{A}^o \mathbf{R}_{\mathbf{dd}}^o (\mathbf{A}^o)^H + \sigma \mathbf{I}, \tag{15}$$

where  $\mathbf{R}_{\mathbf{dd}}^o$  represents the signal correlation matrix formulated by only considering  $n_o$  signals out of the total number of signal arrivals  $n$ .

Let  $\lambda_1^o > \lambda_2^o > \dots > \lambda_{n_o}^o > \lambda_{n_o+1}^o = \lambda_{n_o+2}^o = \dots = \lambda_m^o = \sigma$  denote the eigenvalues of the correlation matrix defined from a data record of a mixture of the  $n_o$  selected FM signals,  $\mathbf{R}_{\mathbf{xx}}^o = \mathbf{A}^o \mathbf{R}_{\mathbf{dd}}^o (\mathbf{A}^o)^H + \sigma \mathbf{I}$ . We also denote  $\lambda_1^{tf} > \lambda_2^{tf} > \dots > \lambda_{n_o}^{tf} > \lambda_{n_o+1}^{tf} = \lambda_{n_o+2}^{tf} = \dots = \lambda_m^{tf} = \sigma^{tf}$  as the eigenvalues of  $\mathbf{D}$  defined in (15). From (15), we have

$$\lambda_i^{tf} = \begin{cases} \frac{L}{n_o}(\lambda_i^o - \sigma) + \sigma = \frac{L}{n_o} \tilde{\lambda}_i^o + \sigma & i \leq n_o \\ \sigma^{tf} = \sigma & n_o < i \leq m, \end{cases} \tag{16}$$

where  $\tilde{\lambda}_i^o \triangleq \lambda_i^o - \sigma$ .

### 3. TIME-FREQUENCY MUSIC

When  $n_o$  signals are selected, the t-f MUSIC determines the angles of the  $n_o$  signals by locating the  $n_o$  peaks of the spatial spectrum defined from the  $n_o$  signals' respective time-frequency regions [4].

$$f_{MU}^{tf}(\theta) = [\mathbf{a}^H(\theta) \hat{\mathbf{G}}^{tf} (\hat{\mathbf{G}}^{tf})^H \mathbf{a}(\theta)]^{-1} = [\mathbf{a}^H(\theta) (\mathbf{I} - \hat{\mathbf{S}}^{tf} (\hat{\mathbf{S}}^{tf})^H) \mathbf{a}(\theta)]^{-1} \tag{17}$$

where  $\mathbf{G}^{tf}$  and  $\mathbf{S}^{tf}$  are the noise and signal subspace estimates obtained from the eigenstructure of matrix  $\mathbf{D}$ . When  $N - L + 1$  points for each of the  $n_o$  FM signals are used in the time-frequency averaging, the variance of the DOA estimates based on t-f MUSIC is given by [9]

$$E(\hat{\omega}_i^{tf} - \omega_i)^2 = \frac{1}{2(N - L + 1)} \frac{\mathbf{a}^H(\theta_i) \mathbf{U}^{tf} \mathbf{a}(\theta_i)}{h^{tf}(\theta_i)}, \tag{18}$$

where  $\omega_i$  is the spatial frequency associated to DOA  $\theta_i$  and  $\hat{\omega}_i^{tf}$  is its estimate obtained by the t-f MUSIC. Moreover,

$$\begin{aligned} \mathbf{U}^{tf} &= \frac{\sigma L}{n_o(N - L + 1)} \left[ \sum_{k=1}^{n_o} \frac{\lambda_k^{tf}}{(\sigma - \lambda_k^{tf})^2} \mathbf{s}_k^{tf} (\mathbf{s}_k^{tf})^H \right] \delta_{i,j} \\ &= \frac{\sigma}{N - L + 1} \left[ \sum_{k=1}^{n_o} \frac{\tilde{\lambda}_k^o + (n_o/L)\sigma}{(\tilde{\lambda}_k^o)^2} \mathbf{s}_k^o (\mathbf{s}_k^o)^H \right] \delta_{i,j} \end{aligned} \tag{19}$$

and

$$h^{tf}(\theta) = \mathbf{c}^H(\theta) \mathbf{G}^{tf} (\mathbf{G}^{tf})^H \mathbf{c}(\theta), \tag{20}$$

with

$$\mathbf{c}(\theta) = d\mathbf{a}(\theta)/d\omega. \tag{21}$$

From (18) and (19), two important observations are in order. First, if the signals are both localizable and separable in the time-frequency domain, then the reduction of the number of signals from  $n$  to  $n_o$  greatly reduces the estimation error, specifically when the signals are closely spaced. The second observation relates to SNR enhancements. The above equations show that error reductions using STFDs are more pronounced for the cases of low SNR and/or closely spaced signals. It is clear from (19) that, when  $\lambda_k^o \gg \sigma$  for  $k = 1, 2, \dots, n_o$ , the results are almost independent of  $L$  (assume  $N \gg L$  so that  $N - L + 1 \simeq N$ ), and therefore there would be no obvious improvement in using the STFD over conventional array processing. On the other hand, when some of the eigenvalues are close to  $\sigma$  ( $\lambda_k^o \simeq \sigma$ , for some  $k = 1, 2, \dots, n_o$ ), which is the case of weak or closely spaced signals, all the results of above three equations are reduced by a factor of up to  $G = L/n_o$ , respectively. This factor represents, in essence, the gain achieved by using STFD processing. To numerically demonstrate the effect of the SNR enhancement, Fig. 2 shows the following normalized factor that is obtained using the  $k$ th term in the summation (19) and its respective value in conventional MUSIC

$$\eta_k = \frac{L}{n_o} \frac{\lambda_k^{tf}}{(\sigma - \lambda_k^{tf})^2} \bigg/ \frac{\lambda_k^o}{(\sigma - \lambda_k^o)^2} = \frac{\tilde{\lambda}_k^o + (n_o/L)\sigma}{\tilde{\lambda}_k^o + \sigma}$$

versus  $\tilde{\lambda}_k^o/\sigma$  for different gain factor  $G = L/n_o$ . This is a key factor in determining the DOA variance of the t-f MUSIC estimates (18). It is evident from this figure that the effect of the gain factor becomes significant at low SNR.

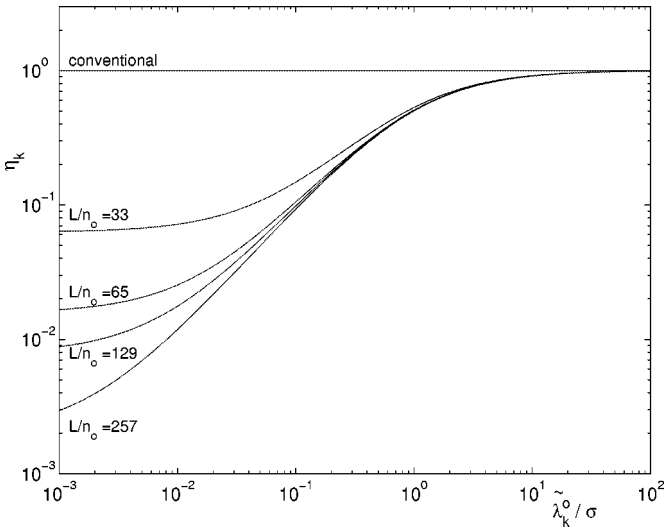


FIG. 2. Normalized factor  $\eta_k$  vs.  $\tilde{\lambda}_k^o/\sigma$ .

## 4. EFFECT OF CROSSTERM DISTRIBUTION

### 4.1. Crossterm Distribution

Crossterms are a by-product of the time-frequency distribution due to its bilinearity. Although different kernels have different ways of mitigating crossterms [14], nevertheless complete removal of crossterms is very difficult to achieve.

There are two sources of crossterms in the underlying direction finding problems. The first type is due to the interactions between the components of the same source signal. These crossterms always reside, along with the autoterms, on the main diagonal of the source TFD matrix. The other type of crossterms is those generated from the interactions between two signal components belonging to two different sources. These crossterms are associated with cross-TFD of the source signals and, at any given time-frequency point, they constitute the off-diagonal entries of the source TFD matrices.

Below, we consider the second type of crossterms. When crossterms are present at the selected time-frequency point, the source TFD takes the following general form,

$$\mathbf{D}_{\mathbf{d}\mathbf{d}}(t, f) = \begin{bmatrix} D_{d_1d_1}(t, f) & D_{d_1d_2}(t, f) & \dots & D_{d_1d_n}(t, f) \\ D_{d_2d_1}(t, f) & D_{d_2d_2}(t, f) & \dots & D_{d_2d_n}(t, f) \\ \vdots & \vdots & \ddots & \vdots \\ D_{d_nd_1}(t, f) & D_{d_nd_2}(t, f) & \dots & D_{d_nd_n}(t, f) \end{bmatrix}, \tag{22}$$

where the off-diagonal element

$$D_{d_i d_j}(t, f) = \sum_{k=-\infty}^{\infty} \sum_{\tau=-\infty}^{\infty} \phi(k, \tau) d_i(t+k+\tau) d_j^*(t+k-\tau) e^{-j4\pi f \tau}$$

is the crossterm of source signals  $d_i(t)$  and  $d_j(t)$  at the point  $(t, f)$ .

#### 4.2. Comparison to Cross-Correlation

To understand the role of crossterms in direction finding, it is important to compare the crossterms to the cross-correlation between signals in conventional array processing, whose properties are familiar. When signals are correlated, the correlation matrix of the source signals is given at the form

$$\mathbf{R}_{\mathbf{d}\mathbf{d}} = \begin{bmatrix} R_{d_1 d_1} & R_{d_1 d_2} & \dots & R_{d_1 d_n} \\ R_{d_2 d_1} & R_{d_2 d_2} & \dots & R_{d_2 d_n} \\ \vdots & \vdots & \ddots & \vdots \\ R_{d_n d_1} & R_{d_n d_2} & \dots & R_{d_n d_n} \end{bmatrix}, \tag{23}$$

where the off-diagonal element

$$R_{d_i d_j} = E[d_i(t) d_j^*(t)]$$

represents the correlation between source signals  $d_i$  and  $d_j$ . Direction finding problems can usually be solved when the signals are partially correlation; however, full rank property of the covariance matrix  $\mathbf{R}_{\mathbf{d}\mathbf{d}}$  is a necessary condition.

Comparing Eqs. (22) and (23), it is clear that the cross-correlation terms and the crossterms have analogous form and similar function. However, the correlation matrix in (23) is defined for stationary signal environments, whereas the matrix in (22) is defined at a  $(t, f)$  point and its value usually varies with respect to time  $t$  and frequency  $f$  under both stationary and nonstationary signal conditions.

When multiple  $(t, f)$  points are incorporated, the effect of a crossterm may be reduced, since the crossterm usually oscillates with respect to time. In the next subsection, we demonstrate this property by using simulation examples.

#### 4.3. Examples

Consider a six-element linear array with half-wavelength interelement spacing, and two chirp signals arrive. The start and end frequencies of the first signal  $d_1(t)$  are  $f_{1s} = 0.1$  and  $f_{1e} = 0.5$ , and those for the second signal  $d_2(t)$  are  $f_{2s} = 0$  and  $f_{2e} = 0.4$ , respectively. The SNR is 10 dB for each signal, and the DOAs of the two signals are  $\theta_1 = -5^\circ$  and  $\theta_2 = 5^\circ$ , respectively. The number of samples is  $N = 256$ . PWVD is used and the window length is  $L = 129$ . Figure 3 shows the PWVD of the mixed signals at the first sensor.

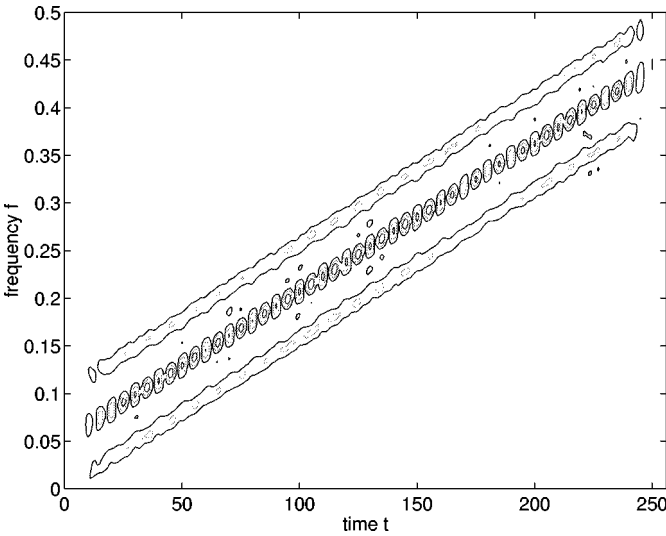


FIG. 3. PWVD of two chirp signals.

The expressions of the signals at the reference array element are given by

$$d_1(t) = \exp[j2\pi(0.1t + 0.2t^2/N)] \quad \text{and} \quad d_2(t) = \exp[j0.4\pi t^2/N], \quad t = 1, 2, \dots, N. \quad (24)$$

The autoterms and the crossterms are obtained as

$$D_{d_1 d_1}(t, f) = \begin{cases} L & f(t) = 0.1 + 0.4t/N \\ \frac{\sin[2\pi L(0.1 + 0.4t/N - f)]}{\sin[2\pi(0.1 + 0.4t/N - f)]} & \text{otherwise} \end{cases} \quad (25)$$

$$D_{d_2 d_2}(t, f) = \begin{cases} L & f(t) = 0.4t/N \\ \frac{\sin[2\pi L(0.4t/N - f)]}{\sin[2\pi(0.4t/N - f)]} & \text{otherwise} \end{cases} \quad (26)$$

$$D_{d_1 d_2}(t, f) = \begin{cases} L \exp[j0.2\pi t] & f(t) = 0.05 + 0.4t/N \\ \frac{\sin[2\pi L(0.05 + 0.4t/N - f)]}{\sin[2\pi(0.05 + 0.4t/N - f)]} \exp[j0.2\pi t] & \text{otherwise} \end{cases} \quad (27)$$

and

$$D_{d_2 d_1}(t, f) = D_{d_1 d_2}^*(t, f). \quad (28)$$

We especially consider the autoterms and the crossterms at the following two regions: (i) autoterm regions  $(t, f_1)$  with  $f_1(t) = 0.1 + 0.4t/N$  and  $(t, f_2)$  with  $f_2(t) = 0.4t/N$ , where the autoterms are dominant; and (ii) crossterm region  $(t, f_c)$  with  $f_c(t) = [f_1(t) + f_2(t)]/2 = 0.05 + 0.4t/N$ , where the crossterm is dominant. Both the autoterm and the crossterm regions have large peak values and are most likely to be selected.

(i) *Autoterm regions.* In the autoterm region of  $d_1(t)$ ,  $(t, f_1)$ , the autoterm of  $d_1(t)$  is constant. The autoterm of  $d_2(t)$  and the crossterm between  $d_1(t)$  and

$d_2(t)$  are relatively small. The source TFD matrices with this region have the form of

$$\mathbf{D}_{\text{ad}}(t, f_1) = \begin{bmatrix} L & o \\ o & o \end{bmatrix}, \tag{29}$$

where  $o$  denotes a negligibly small value. Similar results can be obtained for the autoterm region of  $d_2(t)$ , where the source TFD matrices

$$\mathbf{D}_{\text{ad}}(t, f_2) = \begin{bmatrix} o & o \\ o & L \end{bmatrix}. \tag{30}$$

Since both matrices have dominant diagonal elements with constant values, incorporating only autoterm points, either by joint block-diagonalization or by time-frequency averaging, usually provides good direction finding performance.

(ii) *Crossterm regions.* In this region the crossterms  $D_{d_1d_2}$  and  $D_{d_2d_1}$  are dominant. These crossterms are complex conjugates, and the source TFD matrices within this region take the following form

$$\mathbf{D}_{\text{ad}}(t, f_c) = \begin{bmatrix} o & L \exp(j0.2\pi t) \\ L \exp(-j0.2\pi t) & o \end{bmatrix} \tag{31}$$

which is antidiagonal. Note that unlike a correlation matrix at coherent signal case, which is singular, the above source TFD matrix is still full rank because of the absence of dominant diagonal elements (although the matrix is not necessary positive definite). Accordingly, the noise subspace can be properly estimated, even when only the crossterm points are selected.

However, since the crossterms change with time  $t$ , taking both positive and negative values, averaging them at different  $(t, f)$  points yields small smoothed values. Therefore, incorporating multiple time-frequency points in (31) via time-frequency averaging may lead to degraded performance in some cases. Performing joint block-diagonalization instead of time-frequency averaging avoids such risk.

Figures 4 and 5 show the estimated spatial spectra of the t-f MUSIC by using joint block-diagonalization and time-frequency averaging, respectively, for three independent trials. From top to bottom, the figures show the results by choosing (a) autoterm regions  $f(t) = f_1(t)$  and  $f(t) = f_2(t)$ , (b) crossterm region  $f(t) = [f_1(t) + f_2(t)]/2$ , (c) autoterm and crossterm regions  $f(t) = f_1(t)$ ,  $f(t) = f_2(t)$ , and  $f(t) = [f_1(t) + f_2(t)]/2$ , and (d) autoterm region of the first signal,  $f(t) = f_1(t)$ .

It is seen that both the joint block-diagonalization and time-frequency averaging resolve the signals in the second and third cases, where the crossterm points are included. However, the performance is degraded when using the time-frequency averaging methods. Table 1 shows the standard deviation of the DOA estimates of signal  $d_1(t)$  obtained from 100 independent Monte-Carlo runs. It is evident that the joint block-diagonalization outperforms the time-frequency averaging, particularly when the crossterm region is involved.

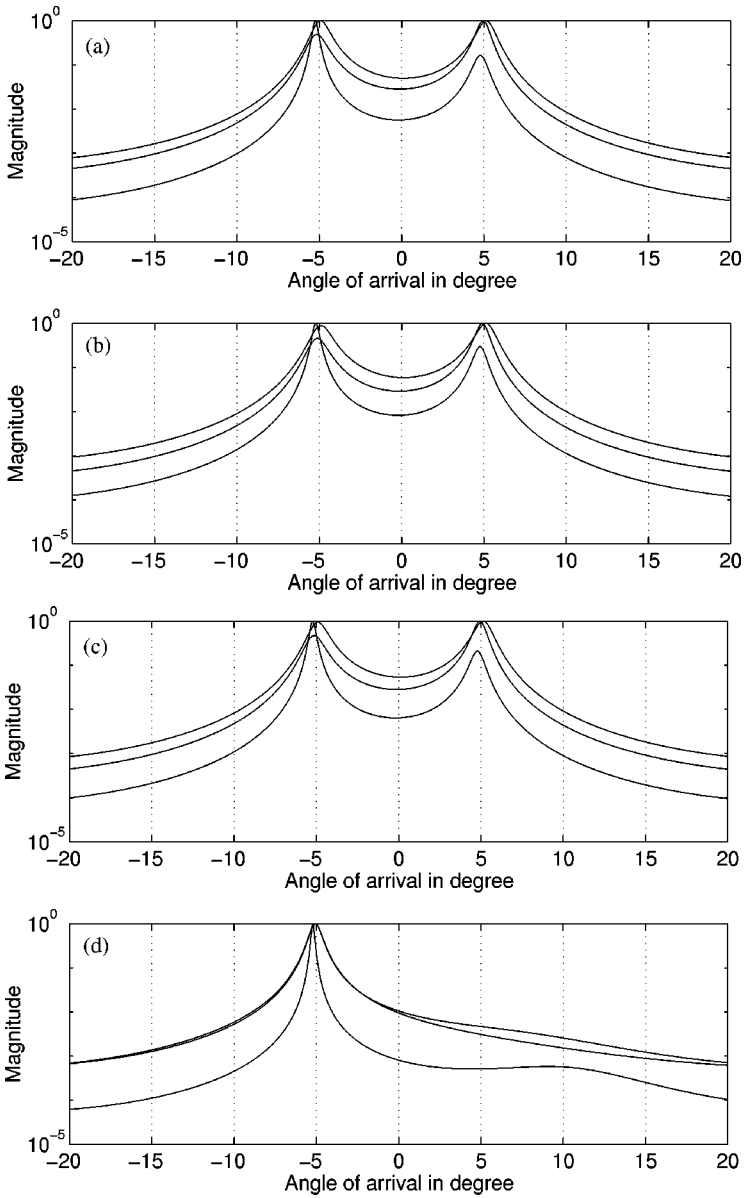


**FIG. 4.** Spatial spectra estimates by using joint block-diagonalization. From top: (a) autoterm regions  $f(t) = f_1(t)$  and  $f(t) = f_2(t)$ , (b) crossterm region  $f(t) = [f_1(t) + f_2(t)]/2$ , (c) autoterm and crossterm regions specified in (a) and (b), and (d) autoterm region of the first signal,  $f(t) = f_1(t)$ .

**TABLE 1**  
Standard Deviation of DOA Estimates

	Case (a)	Case (b)	Case (c)	Case (d)
Joint block-diagonalization	0.156°	0.154°	0.180°	0.121°
Time-frequency averaging	0.179°	0.339°	0.199°	0.161°

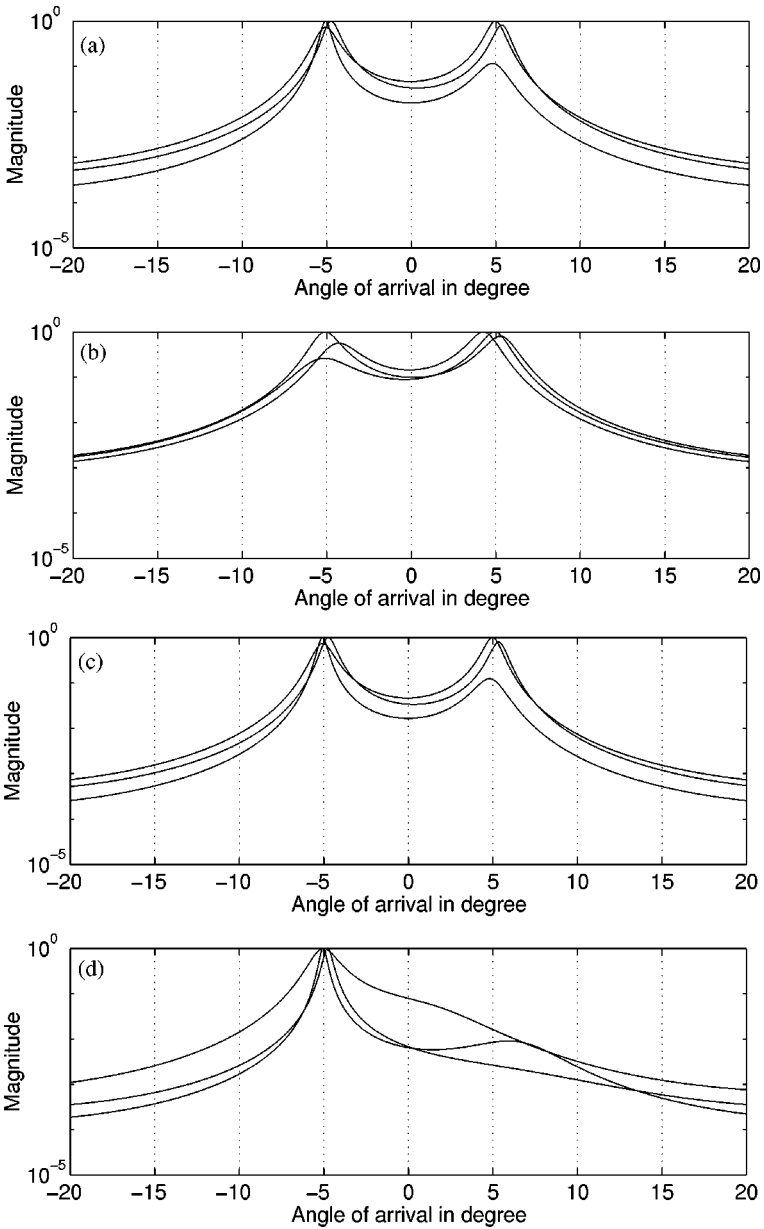


**FIG. 5.** Spatial spectra estimates by using time-frequency averaging. From top: (a) autoterm regions  $f(t) = f_1(t)$  and  $f(t) = f_2(t)$ , (b) crossterm region  $f(t) = [f_1(t) + f_2(t)]/2$ , (c) autoterm and crossterm regions specified in (a) and (b), and (d) autoterm region of the first signal,  $f(t) = f_1(t)$ .

The fourth case in which only one of the two signals is selected has the best performance for both methods of joint block-diagonalization and time-frequency averaging. An interesting observation is that, in the second case, where only the crossterm region is used, the joint block-diagonalization yields second best performance, whereas the time-frequency averaging shows its worst performance. We maintain that the above discussed role of TFD crossterms and

autoterms will not change with FM signal modulations, as it is much dependent on matrix structure and problem formulation.

For comparison, the estimation error corresponding to the Cramer–Rao bound (CRB) is  $0.148^\circ$  for the above example, whereas the standard deviation of the DOA estimates from conventional MUSIC is  $0.149^\circ$  from the same 100 independent runs. As discussed in Section 3, the improvement of time-frequency MUSIC is significant when, due to the discrimination capacity of the algorithm, fewer signals are selected for processing, and/or when the input SNR is low. It is evident that the time-frequency MUSIC with joint block-diagonalization outperforms the classical MUSIC when it operates at only one signal arrival and the variance is lower than the CRB. On the other hand, the improvement is not evident when both the signals are considered to perform time-frequency MUSIC, as the input SNR is relatively high in this case.

It is noted that the crossterm becomes less oscillatory as the time-frequency signatures of the two source signals become closer. When the signals are coherent, the two signals will have identical time-frequency signatures. The crossterms reside on top of the autoterms, and they will no longer oscillate along the crossterm signature. In such a case, the source TFD matrices are singular at each point, and the t-f MUSIC cannot realize high-resolution DOA estimation. In this case, processing methods such as spatial averaging methods [11, 12] should be used. An alternative way is to use the time-frequency maximum likelihood (t-f ML) method introduced in [8].

## 5. CONCLUSIONS

The performance of time-frequency MUSIC has been discussed when multiple time-frequency points representing auto- and crossterms of signal arrivals are considered in spatial time-frequency distributions. The analysis and simulation results have shown that the crossterm regions can be incorporated in direction finding. However, when the time-frequency averaging methods are used, the use of crossterms may degrade the receiver performance.

## REFERENCES

1. Schmidt, R. O., Multiple emitter location and signal parameter estimation, *IEEE Trans. Antennas Propagat.* **34** (1986), 276–280.
2. Wax, M. and Kailath, T., Detection of signals by information theoretic criteria, *IEEE Trans. Acoustics Speech Signal Process.* **33** (1985), 387–392.
3. Belouchrani, A. and Amin, M., Blind source separation based on time-frequency signal representation, *IEEE Trans. Signal Process.* **46** (1998), 2888–2898.
4. Belouchrani, A. and Amin, M., Time-frequency MUSIC, *IEEE Signal Process. Lett.* **6** (1999), 109–110.
5. Cohen, L., *Time-Frequency Analysis*, Prentice Hall, Englewood Cliffs, NJ, 1995.
6. Cardoso, J. F. and Soughoumiac, A., Blind beamforming for non-Gaussian signals, *IEE Proc. F* **140** (1993), 362–370.
7. Sekihara, K., Nagarajan, S., Poeppl, D., and Miyashita, Y., Time-frequency MEG-MUSIC algorithm, *IEEE Trans. Med. Imaging* **18** (1999), 92–97.

8. Zhang, Y., Mu, W., and Amin, M. G., Time-frequency maximum likelihood methods for direction finding, *J. Franklin Institute* **337** (2000), 483–497.
9. Zhang, Y., Mu, W., and Amin, M. G., Subspace analysis of spatial time-frequency distribution matrices, submitted.
10. Lee, H. and Wengrovitz, M., Resolution threshold of beamspace MUSIC for two closely spaced emitters, *IEEE Trans. Acoustics Speech Signal Process.* **38** (1990), 1545–1559.
11. Shan, T. J. and Kailath, T., On spatial smoothing for DOA estimation of coherent sources, *IEEE Trans. Acoustics Speech Signal Process.* **33** (1985), 806–811.
12. Zhang, Y. and Amin, M. G., Spatial averaging of time-frequency distributions for signal recovery in uniform linear arrays, *IEEE Trans. Signal Process.* **48** (2000).
13. Belouchrani, A., Amin, M. G., and Abed-Meraim, K., Direction finding in correlated noise fields based on joint block-diagonalization of spatio-temporal correlation matrices, *IEEE Signal Process. Lett.* **4** (1997), 266–269.
14. Jeong, J. and Williams, W. J., Kernel design for reduced interference distributions, *IEEE Trans. Signal Process.* **42** (1992), 402–412.

---

MOENESS AMIN received his Ph.D. in electrical engineering in 1984 from the University of Colorado, Boulder. He has been on the faculty of the Department of Electrical and Computer Engineering at Villanova University since 1985, where he is now a professor. From 1995 to 1997, Dr. Amin was an Associate Editor of the IEEE Transactions on Signal Processing and a member of the Technical Committee of the IEEE Signal Processing Society on Statistical Signal and Array Processing. He is currently a member of the IEEE Signal Processing Society Technical Committee on Signal Processing for Communications. He was the General Chair of the 1994 IEEE International Symposium on Time-Frequency and Time-Scale Analysis. Dr. Amin is the General Chair of the 2000 IEEE Workshop on Statistical Signal and Array Processing. Dr. Amin is the recipient of the 1997 IEEE Philadelphia Section Service Award and the IEEE Third Millennium Medal. He is also the recipient of the 1997 Villanova University Outstanding Faculty Research Award. He serves on the Committee of Arts and Science of the Franklin Institute. His current research interests are in the areas of time-frequency analysis, spread spectrum communications, smart antennas, and blind signal processing.

YIMIN ZHANG received his M.S. and Ph.D. from the University of Tsukuba, Japan, in 1985 and 1988, respectively. He joined the faculty of the Department of Radio Engineering, Southeast University, China, in 1988. He served as a technical manager at Communication Laboratory Japan in 1995–1997, and as a visiting researcher at ATR Adaptive Communications Research Laboratories, Japan, in 1997–1998. Currently he is a research associate at the Department of Electrical and Computer Engineering, Villanova University. His current research interests are in the areas of array signal processing, space-time adaptive processing, blind signal processing, digital mobile communications, and time-frequency analysis.